
A Kernel Approach for PDE Discovery and Operator Learning

Da Long

School of Computing,
University of Utah, UT

Shandian Zhe

School of Computing,
University of Utah, UT

Nicole Mrvaljević

Department of Applied Mathematics,
University of Washington, WA

Bamdad Hosseini

Department of Applied Mathematics,
University of Washington, WA

Abstract

This article presents a three-step framework for learning and solving partial differential equations (PDEs) using kernel methods. Given a training set consisting of pairs of noisy PDE solutions and source/boundary terms on a mesh, kernel smoothing is utilized to denoise the data and approximate derivatives of the solution. This information is then used in a kernel regression model to learn the algebraic form of the PDE. The learned PDE is then used within a kernel based solver to approximate the solution of the PDE with a new source/boundary term, thereby constituting an operator learning framework. The proposed method is mathematically interpretable and amenable to analysis, and convenient to implement. Numerical experiments compare the method to state-of-the-art algorithms and demonstrate its superior performance on small amounts of training data and for PDEs with spatially variable coefficients.

2021; Willard et al. 2020). Traditionally, PDEs are designed or discovered by experts based on mathematical and physical intuition, a process that relies on human expertise, data, and mathematical analysis. Once the PDE is accepted as a model it is often solved using computer algorithms to simulate a real-world process of interest.

Recent advances in machine learning (ML) along with the abundance of data have led to the idea of automating this workflow, thereby promising computer programs for discovering a PDE from limited and noisy data and solving the discovered PDE to predict the state of a physical system under previously unseen conditions. The goal of this article is to present such a workflow based on recent advances in the theory of kernel methods. Our methodology is robust to noise in the training data and theoretically interpretable.

To be precise, we consider the setting where the solution of a PDE subject to known forcing is observed at a finite set of locations. This solution is further corrupted by noise and constitutes the training data. Then we consider two problems: (a) *Discover the PDE*, i.e., find the algebraic relationship between the partial derivatives of the solution that describes the PDE; (b) *Solve the PDE* subject to previously unseen forcing. Problem (a) is often referred to as *equation discovery* and goes back to the seminal works of Bongard and Lipson 2007; Schmidt and Lipson 2009. More recently it is often tackled by the Sparse Identification of nonlinear Dynamical Systems (SINDy) algorithm of Brunton, Proctor, and Kutz 2016 and its subvariants. Problem (b) is classical in the field of applied mathematics and numerical PDEs. However, classical numerical methods are very intrusive and are often tailored to specific types of PDEs. Recent techniques such as the Physics Informed Neural Networks (PINNs) of Raissi, Perdikaris, and Karniadakis 2019 or the kernel approach of Chen et al. 2021 can circumvent this issue by relaxing the PDE from an equality constraint to a regression misfit term. Problems (a) and (b) together can be viewed as an instance of *operator learning*, where

1 INTRODUCTION

Partial differential equations (PDEs) are ubiquitous in natural sciences such as physics (Riley, Hobson, and Bence 1999), social sciences (Black and Scholes 1973), biology (Edelstein-Keshet 2005) and engineering (Marsden and Hughes 1994; Temam 2001). To some extent, PDEs are the main subject of interest in the field of Physics Informed Learning (PIL); see (Carleo et al. 2019; Karniadakis et al.

one aims to directly learn the infinite-dimensional solution operator of a PDE; the DeepONet algorithm of Lu et al. 2021 and the Fourier Neural Operator (FNO) approach of Li et al. 2020 are state of the art in this context.

Our proposed approach can be summarized in three steps: (1) kernel smoothing is utilized to denoise the training data and compute pertinent partial derivatives of the solution; (2) kernel regression is used to learn the algebraic form of the PDE; (3) the kernel solver of Chen et al. 2021 is used to solve the discovered PDE under new conditions such as a different forcing than those observed in the training data. Step (1) is classical in the field of Gaussian process (GP) regression and can be used by itself as a denoiser for other methods such as SINDy. Our approach is simple to implement and allows for learning of the kernel that will be used in step 3. Step (2) can be viewed as a kernel analogue of SINDy although we do not impose any sparsity assumptions on our features. Using the kernel perspective here allows us to have more flexibility and accommodate more features as well as variable coefficient PDEs. Step (3) is a meshless PDE solver that can handle general nonlinearities and allows us to incorporate the PDE as a soft constraint and still be able to solve the learned equation without having to worry about well-posedness of the learned PDE. Combining steps 1–3 yields an operator learning framework which, compared to state-of-the-art methods, requires significantly less training data by leveraging the knowledge that the operator of interest is the solution map of a PDE.

The rest of the article is organized as follows: Section 2 reviews background material; Section 3 outlines our proposed methodology in detail; Section 4 reviews the relevant literature; Section 5 presents our numerical experiments; and Section 6 summarizes our conclusions.

2 PRELIMINARIES

We collect here some preliminary results and notation that will be used in the remainder of the article.

2.1 General Nonlinear PDEs

Let $\Omega \subset \mathbb{R}^d$ for $d \geq 1$ be a connected domain with boundary $\partial\Omega$. Given a function $u : \Omega \rightarrow \mathbb{R}$ we write $Du = \{u_{x_1}, u_{x_2}, \dots, u_{x_d}\}$ to denote the set of first order partial derivatives of u and similarly write $D^\nu u$ for $\nu > 1$ to denote the set of ν -th order partial derivatives. We consider general families of PDEs of the form

$$\mathcal{P}(\mathbf{x}, u(\mathbf{x}), Du(\mathbf{x}), \dots, D^{M_P}u(\mathbf{x})) = f(\mathbf{x}), \mathbf{x} \in \Omega, \quad (1a)$$

$$\mathcal{B}(\mathbf{x}, u(\mathbf{x}), Du(\mathbf{x}), \dots, D^{M_B}u(\mathbf{x})) = g(\mathbf{x}), \mathbf{x} \in \partial\Omega, \quad (1b)$$

where $\mathcal{P} : \mathbb{R}^{J_P} \rightarrow \mathbb{R}$ and $\mathcal{B} : \mathbb{R}^{J_B} \rightarrow \mathbb{R}$ are nonlinear functions that define the functional relationships between

\mathbf{x} and values of u and its partial derivatives in the interior and boundary of Ω . The dimensions $J_P = J_P(M_P, d)$ and $J_B = J_B(M_B, d)$ are simply the number of partial derivatives of u involved in the definition of the PDE and the boundary condition. The functions $f : \Omega \rightarrow \mathbb{R}$, often referred to as a forcing/source term, and $g : \partial\Omega \rightarrow \mathbb{R}$, the boundary condition, constitute the data of the PDE. In most practical problems, $M_B \leq M_P$ and $\max\{M_P, M_B\}$ denotes the *degree or order* of the PDE. As an example consider the one dimensional second order PDE

$$\begin{aligned} 2xu_x(x) + (1 + x^2)u_{xx}(x) + u^3(x) &= f(x), x \in (0, 1) \\ u(0) &= u(1) = 0. \end{aligned} \quad (2)$$

We directly read

$$\begin{aligned} \mathcal{P}(s_1, s_2, s_3, s_4) &= 2s_1s_3 + (1 + s_1^2)s_4 + s_2^3, \\ \mathcal{B}(t_1, t_2) &= t_2, \end{aligned}$$

where $\mathbf{s} \equiv [x, u(x), u_x(x), u_{xx}(x)] \in \mathbb{R}^4$ and $\mathbf{t} \equiv [x, u(x)] \in \mathbb{R}^2$ and we used bold letters to denote the vectors of the s_i and t_i . Throughout the rest of the article we will assume that whenever a PDE is presented, it is well-defined and has a unique strong solution u , i.e., a solution that is defined pointwise.

2.2 Representer Theorems

Following Muandet et al. 2017, we say that a function $\mathcal{K} : \mathbb{R}^d \times \mathbb{R}^d \rightarrow \mathbb{R}$ is a *Mercer kernel* if it is symmetric ($\mathcal{K}(\mathbf{s}_1, \mathbf{s}_2) = \mathcal{K}(\mathbf{s}_2, \mathbf{s}_1)$) and that for any collection of points $S = \{\mathbf{s}_1, \dots, \mathbf{s}_n\}$ the matrix $(\mathcal{K}(S, S))_{ij} = \mathcal{K}(\mathbf{s}_i, \mathbf{s}_j)$ is positive definite. We write $\mathcal{H}_{\mathcal{K}}$ to denote the Reproducing Kernel Hilbert Space (RKHS) associated to \mathcal{K} with its norm denoted by $\|\cdot\|_{\mathcal{K}}$.

Suppose $\mathcal{H}_{\mathcal{K}} \subset C^\alpha(\mathbb{R}^d)$ with $\alpha \in \mathbb{N}$, the space of real valued functions with α -continuous derivatives, and fix the points $X = \{\mathbf{x}_1, \dots, \mathbf{x}_J\} \subset \mathbb{R}^d$. Let $\delta_j : C^0(\mathbb{R}^d) \rightarrow \mathbb{R}$ denote the pointwise evaluation operator mapping a function $u \in C^0(\mathbb{R}^d)$ to its point value $u(\mathbf{x}_j)$ for $(1 \leq j \leq J)$; let $L_q : C^\alpha(\mathbb{R}^d) \rightarrow C^0(\mathbb{R}^d)$ for $q = 1, \dots, Q$ be bounded and linear operators, and define the maps

$$\phi_j^q := \delta_j \circ L_q, \quad u \mapsto L_q(u)(\mathbf{x}_j),$$

which apply the L_q operators first and then evaluate the output at the points \mathbf{x}_j . For PDE solvers, these maps often evaluate the partial derivatives of u at collocation points. Concatenating the ϕ_j^q along the j and q indices we obtain a vector of maps $\phi : C^\alpha(\mathbb{R}^d) \rightarrow \mathbb{R}^N$, where $N = QJ$. The ordering of the ϕ_j^q is innocuous and henceforth we write ϕ_n for $n = 1, \dots, N$ to denote the entries of the vector ϕ .

We now consider regression problems of the form

$$\underset{u}{\text{minimize}} \|u\|_{\mathcal{K}}^2 + \frac{1}{\lambda^2} \|\mathcal{F} \circ \phi(u) - \mathbf{o}\|_2^2, \quad (3)$$

where $\lambda > 0$ is a parameter, $\mathcal{F} : \mathbb{R}^N \rightarrow \mathbb{R}^O$ is a nonlinear map, and $\mathbf{o} \in \mathbb{R}^O$ is a fixed vector. By Proposition 2.3 of Chen et al. 2021, minimizers $\bar{\mathbf{u}}$ of (3) have the form

$$\bar{\mathbf{u}}(\mathbf{x}) = \mathcal{K}(\mathbf{x}, \phi) \mathcal{K}(\phi, \phi)^{-1} \bar{\mathbf{z}}, \quad (4)$$

where $\mathcal{K}(\mathbf{x}, \phi)$ is a vector field on \mathbb{R}^d with entries $\mathcal{K}(\mathbf{x}, \phi)_i = \phi_i(\mathcal{K}(\mathbf{x}, \cdot))$ for $i = 1, \dots, N$ and $\mathcal{K}(\phi, \phi) \in \mathbb{R}^{N \times N}$ is a symmetric matrix with entries $(\mathcal{K}(\phi, \phi))_{ij} = \phi_i \otimes \phi_j(\mathcal{K})$, i.e., we apply ϕ_i along the first argument of \mathcal{K} then apply ϕ_j along the second argument. The vector $\bar{\mathbf{z}}$ solves the optimization problem

$$\underset{\mathbf{z} \in \mathbb{R}^N}{\text{minimize}} \quad \mathbf{z}^T \mathcal{K}(\phi, \phi)^{-1} \mathbf{z} + \frac{1}{\lambda^2} \|\mathcal{F}(\mathbf{z}) - \mathbf{o}\|_2^2. \quad (5)$$

If $N = O$ and $\mathcal{F} = \text{Id}$ we can solve (5) explicitly to obtain

$$\bar{\mathbf{u}}(\mathbf{x}) = \mathcal{K}(\mathbf{x}, \phi) (\mathcal{K}(\phi, \phi) + \gamma^2 I)^{-1} \mathbf{o}, \quad (6)$$

which is a familiar expression in kernel regression.

3 METHODOLOGY

We now outline our kernel methodology for equation discovery and operator learning of PDEs from empirical data. For simplicity we will only consider the case where the function \mathcal{P} in (1) is unknown since this is most practically relevant. The approach can be extended to learn \mathcal{B} in a similar manner. We will also assume that the degree M_P of the PDE is known.

3.1 Kernel Smoothing of the Training Data

Suppose a set of mesh points $X = \{\mathbf{x}_j\}_{j=1}^J \subset \Omega$ is fixed and let $\{u^{(i)}, f^{(i)}\}_{i=1}^I$ be pairs of solutions and forcing terms for the PDE (1) with the same boundary conditions. Our training data consists of noisy observations of the pairs $(u^{(i)}, f^{(i)})$ at the points X , that is,

$$\begin{aligned} \mathbb{R}^J \ni \mathbf{u}^{(i)} &= u^{(i)}(X) + \epsilon^{(i)}, \\ \mathbb{R}^J \ni \mathbf{f}^{(i)} &= f^{(i)}(X), \end{aligned}$$

where we used the shorthand notation $u(X) = (u(\mathbf{x}_1), \dots, u(\mathbf{x}_J))$ and $\epsilon^{(i)} \sim N(0, \beta^2 I)$ is the measurement noise whose standard deviation β may be unknown.

Our first task is to perform kernel smoothing on the $\mathbf{u}^{(i)}$ to filter out the noise. Using (6) with $\phi_j \equiv \delta_j$ we obtain the smoothed solutions

$$\bar{u}^{(i)}(\mathbf{x}) = \mathcal{U}(\mathbf{x}, X) (\mathcal{U}(X, X) + \beta_{\mathcal{U}}^2 I)^{-1} \mathbf{u}^{(i)}, \quad (7)$$

where \mathcal{U} is a kernel chosen so that $\mathcal{H}_{\mathcal{U}} \subset C^{M_P}(\mathbb{R}^d)$. A simple choice would be the RBF kernel $\mathcal{U}(\mathbf{x}_1, \mathbf{x}_2) = \exp\left(-\frac{1}{2l_{\mathcal{U}}^2} \|\mathbf{x}_1 - \mathbf{x}_2\|_2^2\right)$ whose RKHS consists of infinitely smooth functions; although this kernel may result in overly

smoothed training data. Another natural choice is the Matérn family of kernels (see Genton 2001) that allow precise control over the smoothness class of the observed solutions. The noise standard deviation (nugget) $\beta_{\mathcal{U}}^2 > 0$ and the kernel parameters $l_{\mathcal{U}}$ can be tuned using hyperparameter tuning methods such as cross validation (CV) or maximum likelihood (MLE).

We proceed by differentiating (7) to approximate the derivatives of $u^{(i)}$,

$$D^\nu \bar{u}^{(i)}(\mathbf{x}) = D^\nu \mathcal{U}(\mathbf{x}, X) (\mathcal{U}(X, X) + \beta_{\mathcal{U}}^2 I)^{-1} \mathbf{u}^{(i)}.$$

We then evaluate the derivatives at the mesh points X for $\nu \leq M_P$ to define the vectors

$$\mathbf{s}_j^{(i)} = \left(\mathbf{x}_j, \bar{u}^{(i)}(\mathbf{x}_j), D\bar{u}^{(i)}(\mathbf{x}_j), \dots, D^{M_P} \bar{u}^{(i)}(\mathbf{x}_j) \right).$$

The pairs $(\mathbf{s}^{(i)}, \mathbf{f}^{(i)})$ constitute our training data for equation discovery.

3.2 Discovering the PDE

Assuming that $D^\nu \bar{u}^{(i)}$ are close to $D^\nu u$ we can substitute \bar{u} in (1a) and evaluate at the points $\mathbf{x}_j \in X$ to write

$$\mathcal{P}(\mathbf{s}_j^{(i)}) = f^{(i)}(\mathbf{x}_j).$$

We view these identities as interpolation constraints for the function \mathcal{P} and use them to define a kernel interpolant $\bar{\mathcal{P}}$. More precisely, let $\mathcal{K} : \mathbb{R}^{J_P} \times \mathbb{R}^{J_P} \rightarrow \mathbb{R}$ be a Mercer kernel and write $S = \{\mathbf{s}^{(1)}, \dots, \mathbf{s}^{(I)}\}$ and $\mathbf{f} = (\mathbf{f}^{(1)}, \dots, \mathbf{f}^{(I)})$. We can then use (3) to write

$$\bar{\mathcal{P}}(\mathbf{s}) = \mathcal{K}(\mathbf{s}, S) (\mathcal{K}(S, S) + \beta_{\mathcal{K}}^2 I)^{-1} \mathbf{f}. \quad (8)$$

The parameter $\beta_{\mathcal{K}} > 0$ is a nugget that can be tuned to stabilize the inversion of the kernel matrix $\mathcal{K}(S, S)$. For our experiments we will take \mathcal{K} to be the RBF kernel to have maximum flexibility and accommodate variable coefficients¹. The length scale parameter $l_{\mathcal{K}}$ of the kernel \mathcal{K} can once again be tuned using standard hyperparameter tuning methods.

3.3 Solving the Discovered PDE

In the third and final step of our methodology we aim to solve the PDE defined by the function $\bar{\mathcal{P}}$ for a new source term \tilde{f} . More precisely, we wish to find \tilde{u} that solves

$$\begin{aligned} \bar{\mathcal{P}}(\mathbf{x}, \tilde{u}(\mathbf{x}), D\tilde{u}(\mathbf{x}), \dots, D^{M_P} \tilde{u}(\mathbf{x})) &= \tilde{f}(\mathbf{x}), \quad \mathbf{x} \in \Omega, \\ \mathcal{B}(\mathbf{x}, \tilde{u}(\mathbf{x}), D\tilde{u}(\mathbf{x}), \dots, D^{M_B} \tilde{u}(\mathbf{x})) &= g(\mathbf{x}), \quad \mathbf{x} \in \partial\Omega. \end{aligned}$$

¹Another possible choice is the polynomial kernel whose features are polynomials of a certain degree. This kernel is closely associated with the SINDy algorithm.

We will follow the approach of Chen et al. 2021 for this step. We only outline the main idea of the solver here and refer to that paper for details.

We will approximate the solution \tilde{u} by looking for a function in the RKHS $\mathcal{H}_{\mathcal{U}}^2$ that satisfies the PDE at a set of collocation points. Let $\{\tilde{\mathbf{x}}_1, \dots, \tilde{\mathbf{x}}_{\tilde{J}_\Omega}\} \subset \Omega$, a set of interior collocation points, and $\{\tilde{\mathbf{x}}_{\tilde{J}_\Omega+1}, \dots, \tilde{\mathbf{x}}_{\tilde{J}}\} \subset \Omega$, the boundary collocation points. Then Chen et al. 2021, proposed an algorithm for solving

$$\begin{aligned} & \underset{u}{\text{minimize}} \quad \|u\|_{\mathcal{U}}^2 \\ & + \frac{1}{\lambda_{\mathcal{P}}^2} \sum_{j=1}^{\tilde{J}_\Omega} |\overline{\mathcal{P}}(\tilde{\mathbf{x}}_j, \dots, D^{M_P} u(\tilde{\mathbf{x}}_j)) - \tilde{f}(\tilde{\mathbf{x}}_j)|^2 \\ & + \frac{1}{\lambda_{\mathcal{B}}^2} \sum_{j=\tilde{J}_\Omega+1}^{\tilde{J}} |\mathcal{B}(\tilde{\mathbf{x}}_j, \dots, D^{M_B} u(\tilde{\mathbf{x}}_j)) - g(\tilde{\mathbf{x}}_j)|^2, \end{aligned} \quad (9)$$

and showed that, under appropriate conditions, the minimizer of this problem converges to \tilde{u} as the number of collocation points $\tilde{J} \rightarrow \infty$ and the regularization parameters $\lambda_{\mathcal{P}}, \lambda_{\mathcal{B}} \rightarrow 0$. By identifying the appropriate maps ϕ , depending on the partial derivatives that are involved in defining the PDE, one can identify the minimizer \tilde{u} of (9) via (4) with the vector \mathbf{z} solving the optimization problem

$$\begin{aligned} & \underset{\mathbf{z}}{\text{minimize}} \quad \mathbf{z}^T \mathcal{U}(\phi, \phi)^{-1} \mathbf{z}^T \\ & + \frac{1}{\lambda_{\mathcal{P}}^2} \sum_{j=1}^{\tilde{J}_\Omega} |\overline{\mathcal{P}}(\mathbf{z}_j) - \tilde{f}(\tilde{\mathbf{x}}_j)|^2 \\ & + \frac{1}{\lambda_{\mathcal{B}}^2} \sum_{j=\tilde{J}_\Omega+1}^{\tilde{J}} |\mathcal{B}(\mathbf{z}_j) - g(\tilde{\mathbf{x}}_j)|^2, \end{aligned} \quad (10)$$

where $\mathbf{z} = (\mathbf{z}_1, \dots, \mathbf{z}_{\tilde{J}})$ is obtained by concatenating the \mathbf{z}_j . The entries of the vectors \mathbf{z}_j corresponds to the values of u and its pertinent derivatives $D^\nu u$ evaluated at the collocation points $\tilde{\mathbf{x}}_j$. The optimization problem for \mathbf{z} is solved using the Gauss-Newton iteration. The entries of the kernel matrix $\mathcal{U}(\phi, \phi)$ are obtained by evaluating $\phi_i \otimes \phi_j(\mathcal{U})$ as outlined in Section 2.2. This requires application of differential operators to kernels before evaluating them at the collocation points. The differentiation can be done using symbolic calculation software or automatic differentiation. For additional stability a nugget term may be added to the kernel matrix $\mathcal{U}(\phi, \phi)$ to further stabilize the Gauss-Newton iterations.

²One can choose a different kernel, say $\tilde{\mathcal{U}}$, or different kernel parameters $l_{\mathcal{U}}$ for this step. However, it is natural to use the same kernel as in the kernel smoothing step since, if the training data is sufficient, we expect to be able to learn the optimal kernel parameters $l_{\mathcal{U}}$ in that step.

4 RELATED WORK

Identifying the parameters of a differential equation (DE) is a well-known inverse problem; see the works of Bock 1981, 1983 on parameter identification of ordinary differential equations (ODEs) as well as the book of Kaipio and Somersalo 2006 and the article of Stuart 2010 for examples involving PDEs. Such problems are also encountered in optimal control of PDEs as outlined in the book of Tröltzsch 2010. However, these classic approaches operate under the assumption that the expression of the DE is known up to free parameters that need to be identified from experimental data. Indeed, the approach of Chen et al. 2021 readily extends to solving such inverse problems.

Equation discovery/learning is a more recent problem attributed to Bongard and Lipson 2007; Schmidt and Lipson 2009 who used symbolic regression to discover underlying physical laws from experimental data. Compared with the aforementioned inverse problems, the goal here is to discover the very form of the DE as well as its parameters from experimental data. DEs that describe real world physical systems involve only a few terms and often have simple expressions. Based on this philosophy, recent approaches to equation learning try to learn a DE (i.e., the function \mathcal{P} in our formulation) from a dictionary of possible terms/features along with a sparsity assumption to ensure only a few terms will be active. Perhaps the best known example of such an approach is the SINDy algorithm of Brunton, Proctor, and Kutz 2016; Rudy et al. 2017. SINDy has been expanded in many directions ever since (see Silva et al. 2020 and references within) and other authors have considered similar approaches (Kang, Liao, and Liu 2021; Schaeffer 2017). At a high level, the differences between these approaches are in the formulation of the symbolic regression problem and the implementation of a sparsity assumption on the features (L_1, L_0 regularization or various thresholding methods) as well as how they deal with noise in the training data.

Contrary to the feature map perspective of SINDy-type methods, our approach employs a kernel perspective towards learning \mathcal{P} . As a result, we give up the immediate interpretability of the learned function $\overline{\mathcal{P}}$ in favor of more features and a more convenient computational framework that is also able to deal with more general PDEs, such as those involving spatial or temporally varying parameters. Feature based methods often cannot deal with such problems since the construction of appropriate features may require prior knowledge of the general form of the variable coefficients. Our method can also be combined with the kernel mode decomposition approach of Owhadi, Scovel, and Yoo 2021 to extract the dominant features in the learned function $\overline{\mathcal{P}}$, thereby making our approach more interpretable. Additionally, our method opens the door for analyzing the accuracy and robustness of the estimator $\overline{\mathcal{P}}$. Such theoretical ques-

tions have attracted attention very recently (He, Zhao, and Zhong 2022; He et al. 2022) but current theoretical results are quite scarce.

While previous methods find good approximations to \mathcal{P} , the DE that they learn can be very difficult to solve using conventional techniques such as finite differences or finite elements. Simply put, the dictionary of features can involve highly nonlinear and stiff terms that lead to numerical instabilities and may need dedicated solvers. The kernel PDE solver of Chen et al. 2021 alleviates these difficulties since it only relies on knowing the function $\bar{\mathcal{P}}$ and the order of the PDE. We note that one can replace our kernel solver in the final step with other flexible PDE solvers that only rely on knowledge of the algebraic form of the DE, such as the PINNs of Raissi, Perdikaris, and Karniadakis 2019.

Finally, we note that our three-step approach to smoothing the data, learning the PDE, and solving the learned PDE, can be viewed as a semi-explicit approach to operator learning. More precisely, our framework provides an algorithm for approximating the solution of a PDE given a new source or boundary data, from a training set of example solutions to the PDE. To the best of our knowledge this is a novel approach to operator learning which departs from techniques such as the DeepONets of Lu et al. 2021 or the FNO of Li et al. 2020. These methods directly approximate the infinite-dimensional solution map of the PDE using neural networks, effectively ignoring the algebraic form of the PDE. Our method is both computationally and conceptually simpler and requires significantly less training data as demonstrated by the experiments below.

5 EXPERIMENTS

Below we compare our computational framework to state-of-the-art algorithms for equation discovery and operator learning. Three benchmark DEs were considered: a pendulum model (11), a nonlinear diffusion PDE (12) and the Darcy flow PDE (13). Our method was compared to the SINDy algorithm for the equation discovery task and the DeepONet algorithm for the operator learning on these examples³. For our solver we used the implementation of Chen et al. 2021 (<https://github.com/yifanc96/NonLinPDEs-GPsolver>). For estimation of derivatives in our method and the training of DeepONets we used Jax. We used Python to implement SINDy with NumPy for the least squares step.

Common Structure: For each benchmark our method for learning the equation (i.e., computing $\bar{\mathcal{P}}$) was compared to the SINDy algorithm with iterative thresholding proposed by Rudy et al. 2017. Both our method and SINDy were trained using the same training data with our kernel

smoothing method from Section 3.1 used to denoise the training data and to compute the relevant partial derivatives of the $u^{(i)}$. The kernel parameters in this step were tuned using CV. The test error of the learned functions $\bar{\mathcal{P}}$ was computed for our method and SINDy for the pendulum and diffusion examples. The test data set was constructed by taking the same source terms $f^{(i)}$ from the training set and perturbing in a controlled way (see Section 5.1 for details.) The DE was then solved with the perturbed forcing terms and the perturbed solutions were used to generate a testing set for the learned equations. These results are presented in Figure 1 where the parameter β controls the size of the perturbation introduced to the forcing terms. The Darcy flow PDE was excluded from this experiment since SINDy was not applicable.

For operator learning we used the $\bar{\mathcal{P}}$ functions learned using our approach within the solver of Section 3.3 to predict the solution of the equations for 20 new forcing terms. The solver uses the same kernel that was learned in the kernel smoothing step. We performed the same experiments with the function $\bar{\mathcal{P}}$ learned by SINDy but we solved the resulting DE with an independent solver in the pendulum example while our kernel solver was used for the diffusion example. The DeepONet algorithm of Lu et al. 2021 was also trained on the same training data to learn a mapping from the forcing f to the solution u . For each new test forcing we compared the predicted solution of all three methods to a ground truth solution computed using a high-resolution independent solver. The Average test MSEs and their standard deviation for this task are reported in Table 1.

Takeaways: Our experiments are focused on the two distinct but related tasks of equation discovery and operator learning. Our results concerning equation discovery led to three primary observations: (a) kernel smoothing is a good pre-processing step for denoising and estimation of gradient information before learning DEs for both SINDy and our approach. (b) The accuracy and robustness of SINDy is closely tied to the chosen dictionary of functions and the complexity of the underlying problem while our kernel approach appears to perform more consistently across multiple problems. On the other hand, SINDy is able to learn the equation globally under the right circumstances while our method appears to learn the equation locally. (c) SINDy is sensitive to noise in the training data and this sensitivity is not always alleviated by denoising.

Our results concerning operator learning led to two primary observations: (a) In the regime of small training data, operator learning via equation discovery outperforms more general methods such as DeepONets that learn high-dimensional maps between function spaces. This is not surprising since our approach uses explicit knowledge of the fact that the map of interest is the solution operator of a differential equation. We also note that this approach

³SINDy was not used for the Darcy flow PDE since it involves spatially variable coefficients

is possible thanks to the solver of Chen et al. 2021 since equation discovery algorithms can easily lead to ill-posed or unstable equations that cannot be solved by conventional solvers. (b) Algorithms that are more accurate and robust at the equation discovery step also perform better for operator learning independent of the employed solver.

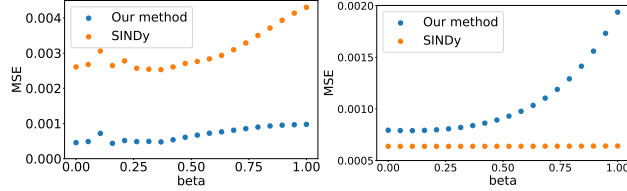


Figure 1: Test error of the learned function $\bar{\mathcal{P}}$ with our method vs. SINDy for the pendulum ODE (left) and the nonlinear diffusion PDE (right). The parameter β controls the departure of the test and training forcing terms.

Method	Pendulum	Diffusion	Darcy Flow
Our method	$4.3e^{-5} (1.3e^{-5})$	$3.4e^{-5} (1.1e^{-5})$	$9.2e^{-7} (2.0e^{-7})$
SINDy	$2.0e^{-4} (1.3e^{-4})$	$1.6e^{-5} (3.0e^{-6})$	N/A
DeepONet	$2.4e^{-2} (7.1e^{-3})$	$1.7e^{-1} (2.4e^{-2})$	$1.1e^{-5} (3.3e^{-6})$

Table 1: Average MSEs for the operator learning task computed for 20 test forcing functions. Standard deviations are reported in brackets

5.1 Pendulum

The following system of ODEs modeling the motion of a pendulum was considered

$$\begin{aligned} (u_1)_t(t) &= u_2(t), \\ (u_2)_t(t) &= -k \sin(u_1(t)) + f(t), \end{aligned} \quad (11)$$

subject to $u_1(0) = u_2(0) = 0$. Note that here we used the parameter t as our input parameter rather than just x as is customary in ODE and PDE literature. The training data for this experiment consists of the pairs of solutions and forcing functions $(u^{(i)}(t_j), f^{(i)}(t_j))$ for $i = 1, \dots, 5$. The points t_j were uniformly distributed over the interval $[0, 1]$ for $j = 1, \dots, 10$. Each forcing $f^{(i)}$ is a random draw from a GP with the RBF kernel and length scale 0.2; see Figure 2. The solutions $u^{(i)}$ corresponding to each forcing were computed using the SciPy solve_ivp function on a fine grid and sub-sampled over the t_j 's.

Equation Discovery: The function $\bar{\mathcal{P}}$ was learned using the methodology of Section 3 with \mathcal{U} taken to be the RBF kernel with length scale 1 for the first coordinate and 0.45 for the second coordinate, and $\beta_{\mathcal{U}}^2 = 10^{-6}$. As for the kernel \mathcal{K} we also chose the RBF kernel with length scale 12 and nugget term $\beta_{\mathcal{K}}^2 = 10^{-6}$. For SINDy we used the dictionary $\{u_2(t), (u_1)_x\}$ to approximate the right hand side (rhs) of the first equation and

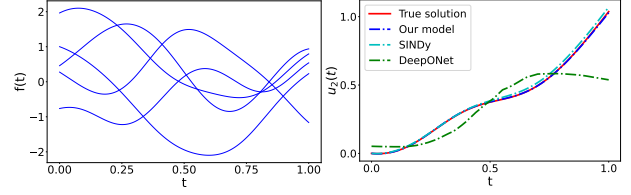


Figure 2: (Left) the forcing terms used to generate the training data for the pendulum ODE. (Right) comparing the ODE solutions obtained for one of the test forcing terms.

$\{f(t), u_1(t), (u_2)_x, u_1^2, u_1^3, \sin(u_1(t)), \cos(u_1(t))\}$ for the rhs of the second equation. We used sequential thresholding at levels $1e^{-1}, 1e^{-2}, 1e^{-3}$ and $1e^{-4}$.

For testing, the forcing terms $f^{(i)}$ from the training set were perturbed as $f^{(i)}(t) + \beta \sin(5\pi t)$.

The corresponding system of ODEs was then solved using this new forcing and the subsequent perturbed solutions $u^{(i)}$ were computed on a grid of 1000 points on the interval $[0, 1]$. Kernel smoothing was used, following Section 3.1, to estimate the pertinent derivatives of the perturbed solutions which were then used to define a new set of inputs over which the error between $\bar{\mathcal{P}}$ and \mathcal{P} was computed. These results are reported in Figure 1. In this example we observe that our approach outperforms SINDy by a factor of 5. This is most likely due to the additional flexibility of the RBF kernel compared to the dictionary of functions. The test errors for both methods increase as a function of β as expected. This is a sign that the function $\bar{\mathcal{P}}$ was learned locally around the training data. When the test points deviate from the training set the quality of $\bar{\mathcal{P}}$ deteriorates, a behavior that is well-understood in the context of kernel regression and interpolation.

Operator Learning: The function $\bar{\mathcal{P}}$ learned by our method was plugged into the solver of Section 3.3 to solve the ODE for a test set of forcing terms. The same kernel \mathcal{U} as the smoothing step was used. We used 9 collocation points on the interval $(0, 1]$ with one point used at $t = 0$ to impose the initial conditions and took $\lambda_{\mathcal{P}}^2 = \lambda_{\mathcal{B}}^2 = 1e^{-8}$. The minimizer of (10) was approximated using 15 iterations of the Newton algorithm introduced in Chen et al. 2021. The equation discovered by SINDy was solved using the solve_ivp function from SciPy. A DeepONet was also trained on our training data to predict u_2 (it is redundant to train the mapping for u_1 since it can be obtained by integrating u_2). Our DeepONet consisted of a four layer branch net of width $10 - 10^3 - 10^3 - 10^3$ and a trunk net of size $1 - 10^3 - 10^3 - 10^3$. Training was performed for 5×10^4 iterations of the Adam optimizer with step size 10^{-3} .

For testing, 20 forcing functions were drawn from the same GP as the training set and the solutions were computed by the independent solver. Figure 3 shows an example of the

predicted solutions for one of our test forcing functions. Test MSEs averaged over the 20 test solutions are reported in Table 1. Our method outperforms SINDy by over an order of magnitude due to the fact that we obtain a more accurate $\bar{\mathcal{P}}$. DeepONet appears to perform significantly worse compared to the other methods, most likely due to the small size of the training set.

We also repeated our experiments by adding noise to the training data. The noise was added at two levels: First, the exact solutions for the training forcing terms were computed, smoothed, and differentiated. Then Gaussian noise was added to the point values of the solutions and their derivatives. Second, Gaussian noise was added to the forcing terms in the training data set. The operator learning test error of our method and SINDy with this noisy training set, are compared in Table 2. The parameter β is the noise to signal ratio of the added noise. DeepONet was not considered since its performance in the previous setting was not competitive. We observe that SINDy is very sensitive to noise in the training set and the results become unreliable quickly while our approach appears robust.

Method	Beta=0.05	Beta=0.10	Beta=0.20
Our method	$2.5e^{-3}(8.7e^{-4})$	$7.1e^{-3}(1.6e^{-3})$	$2.1e^{-2}(7.3e^{-3})$
SINDy	$3.3e^{-1}(1.4e^{-1})$	$1.4(2.9e^{-1})$	$7.0(1.1)$

Table 2: Comparing the test MSEs of our approach and SINDy for operator learning with different levels of noise in the training data for the pendulum ODE. Standard deviations are reported in brackets. Larger values of β correspond to more noise.

5.2 Nonlinear Diffusion PDE

The following second order nonlinear PDE was considered for our second set of experiments

$$u_t(x, t) = 0.01u_{xx}(x, t) + 0.01u^2(x) + f(x), \quad (12)$$

$$(x, t) \in (0, 1) \times (0, 1],$$

subject to boundary conditions $u(0, t) = u(1, t) = 0$ for $t \in (0, 1]$ and initial conditions $u(x, 0) = 0$, for $x \in (0, 1)$. Similar to Section 5.1, the training data was generated by drawing four random sources $f^{(i)}(x)$ from a GP with the RBF kernel and length scale 0.3; note that f is only a function of x here and hence a one dimensional function. As a benchmark PDE solver in this example we used the same finite-difference solver used by Lu et al. 2021. The solution for each forcing was computed on a fine grid of points before they were subsampled to a space-time grid of size 15×15 , constituting the training set.

Equation Discovery: The training data was pre-processed using our kernel smoothing approach with the kernel \mathcal{U} taken to be the RBF kernel with length scale 0.53 and nugget $\beta_{\mathcal{U}}^2 = 10^{-10}$ chosen via CV.

The function $\bar{\mathcal{P}}$ was learned using our approach with \mathcal{K} taken to be the RBF kernel with length scale 20.01 and nugget $\beta_{\mathcal{K}}^2 = 10^{-6}$ chosen via CV. The SINDy algorithm was used to learn the PDE with the dictionary $\{u, u_t, u_{xx}, u^2, u^3, u_{xx}u, u_{xx}u^2, u_{xx}u^3, f, 1\}$. We used the same threshold levels as the pendulum example.

For testing we repeated the same experiment as the pendulum example by considering perturbed source terms $f^{(i)}(x) + \beta \sin(5\pi x)$, i.e., we introduced perturbations in the x variable and sources remained constant in the t direction. We solved the PDE with the independent solver and the perturbed sources and evaluated the solutions on a finer space-time grid of size 50×50 constituting the test set for our equation learning step. Figure 1 compares the error of the learned $\bar{\mathcal{P}}$ for our method and SINDy as a function of the perturbation parameter β . Interestingly, in this example we observe that SINDy is more accurate and more robust than our approach. We attribute this behavior to a good choice of a dictionary which enables SINDy to learn a good global approximation to \mathcal{P} while our approximation remains local. We highlight that for small values of β the difference between the two methods is minimal.

Operator Learning: Similar to the pendulum example we also considered the performance of our method, SINDy, and DeepONet for the diffusion PDE. A test set of 20 new forcing terms were drawn from the same GP used to generate the training set. The test forcing terms were used in the independent solver to approximate the solution of the PDE on a uniform space-time grid of size 50×50 . The kernel PDE solver was used with our equation discover approach and SINDy with a set of uniform set of 15×15 collocation points (43 points on the boundary and 169 points in the interior) with the same kernel \mathcal{U} that was tuned in the kernel smoothing of the training set. The solutions were then compared to the test solutions on a fine grid of size 50×50 points. The DeepONet was trained using a four layer branch net of size $225 - 10^3 - 10^3 - 10^3$ and trunk net of size $2 - 10^3 - 10^3 - 10^3$ and over 10^5 iterations of the Adam optimizer with step size 10^{-3} .

Table 1 summarizes the training performance of the three approaches for the diffusion PDE. Once again we observe that DeepONet is not competitive, however, SINDy obtains slightly better test error compared to our kernel approach. This is expected following Figure 1 and the superior performance of SINDy in identifying the underlying PDE. We repeated this experiment by adding noise to the training data following the same recipe as the pendulum example; see Table 3. We observe that in this case our method and SINDy have nearly identical performance with SINDy having a slight edge. The performance of both methods deteriorates as the level of noise in the training data increases. An example of the predicted solutions on the test set is depicted in Figure 3.

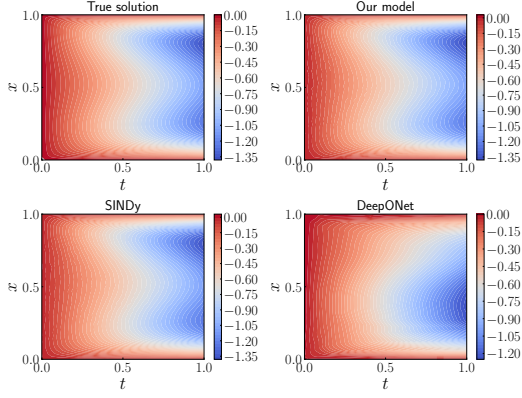


Figure 3: A comparison of the estimated solutions to the diffusion PDE for one of the forcing terms in the test set.

Method	Beta=0.05	Beta=0.10	Beta=0.20
Our method	$3.7e^{-4}(1.1e^{-4})$	$7.2e^{-4}(2.4e^{-4})$	$4.1e^{-3}(1.5e^{-3})$
SINDy	$1.5e^{-4}(4.4e^{-5})$	$4.2e^{-4}(1.3e^{-4})$	$2.7e^{-3}(1.0e^{-3})$

Table 3: Comparing the test MSEs of our approach and SINDy for operator learning with different levels of noise in the training data for the diffusion PDE. Standard deviations are reported in brackets. Larger values of β correspond to more noise.

5.3 Darcy Flow

For our third and final example we considered the Darcy flow PDE

$$-\operatorname{div}(a\nabla u)(x) = f(x), \quad x \in (0,1)^2, \quad (13)$$

subject to homogeneous Dirichlet boundary conditions. The coefficient a is a spatially variable field given by

$$a(x) = \exp(\sin(\pi x_1) + \sin(\pi x_2)) + \exp(-\sin(\pi x_1) - \sin(\pi x_2)).$$

In this experiment we did not consider the SINDy algorithm since the construction of an appropriate dictionary for PDEs with spatially variable coefficients is *not* possible without prior knowledge of the form of a ⁴. Instead we focus primarily on the operator learning problem.

Our experiments follow a similar setup to the previous problems. The training set was generated by drawing four forcing terms from a GP with the RBF kernel and length scale 0.3 along the x_1 coordinate and constant along the x_2 coordinates. For each forcing function the PDE was solved using a standard finite difference solver on a fine uniform grid before the solutions and the corresponding forcing functions were subsampled to a uniform 12×12 grid constituting our training set.

⁴The general problem of interest here is when a is unknown, for example a random field.

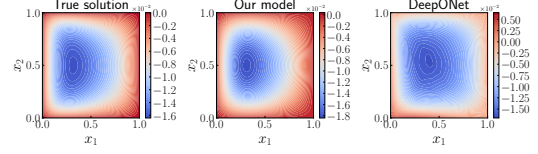


Figure 4: A comparison of the estimated solutions to the Darcy flow PDE for one of the forcing terms in the test set.

Operator Learning: Kernel smoothing was applied to the training data with the RBF kernel \mathcal{U} and with length scale parameter 0.39 and nugget $\beta_{\mathcal{U}}^2 = 10^{-10}$ obtained from CV. The function \mathcal{P} was then learned with \mathcal{K} taken to be the RBF kernel with length scale 2.1 and nugget $\beta_{\mathcal{K}}^2 = 9$.

For testing we drew 20 new forcing functions from the same GP as above but this time we solved the PDE on a uniform grid of size 50×50 . We solved our discovered equation using the kernel PDE solver with a set of 12×12 collocation points (44 points on the boundaries and 100 points in the interior) with the same kernel \mathcal{U} that was tuned in the kernel smoothing step. The solutions were then compared to the test set on the finer grid. We observed that for this experiment the solver was more sensitive to the choice of the $\lambda_{\mathcal{P}}$ and $\lambda_{\mathcal{B}}$ parameters and we had to tune these parameters for each source term in order for the Gauss-Newton iterations to converge. Subsequently, a DeepONet was trained on the same training set with a branch net of size $144 - 10^3 - 10^3 - 10^3$ and trunk net of size $2 - 10^3 - 10^3 - 10^3$ and with 10^5 iterations of the Adam optimizer with step size 10^{-4} . A sample of the predicted solutions in the test set is depicted in Figure 4 while training MSEs are reported in Table 1. Once again we observe that our approach for operator learning outperforms DeepONet although in this case the performance gap appears to be smaller.

6 CONCLUSION

A computational framework was presented for the discovery of DEs and operator learning of their solution maps based on kernel methods. Our method utilized kernel regressions at every step constituting a complete workflow for pre-processing and smoothing of the input data, discovering the DE, and solving it with a new forcing term. Comparison with state-of-the-art algorithms demonstrated that our method for equation discovery is competitively accurate and robust to noise while remaining applicable in broader settings such as PDEs with variable coefficients. For operator learning our method is significantly more data efficient when compared to general neural net based methods that learn mappings between function spaces. Furthermore, our kernel smoothing and PDE solvers can be paired with other equation discovery algorithms such as SINDy to help stabilize those methods and enable operator learning.

Our method is not only competitive but also amenable to theoretical analysis and opens the door for developing theory for equation discovery. For example, our results in Figure 1 show that we learn the algebraic form of the PDE locally around the test data, as expected by the error analysis of kernel regression and scattered data approximation. The correspondence between kernel methods and GPs also suggests a probabilistic perspective towards equation discovery and operator learning, which to our knowledge, has not been explored.

Acknowledgements

The authors would like to dedicated this article to Prof. Nilima Nigam in celebration of her 50th birthday. DL and SZ thank NSF CAREER Award IIS-2046295 and MURI AFOSR grant FA9550-20-1-0358. BH is supported by the NSF grant DMS-2208535.

References

- Black, Fischer and Myron Scholes (1973). “The pricing of options and corporate liabilities”. In: *Journal of political economy* 81.3, pp. 637–654.
- Bock, Hans G (1981). “Numerical treatment of inverse problems in chemical reaction kinetics”. In: *Modelling of chemical reaction systems*. Springer, pp. 102–125.
- (1983). “Recent advances in parameter identification techniques for ode”. In: *Numerical treatment of inverse problems in differential and integral equations*, pp. 95–121.
- Bongard, Josh and Hod Lipson (2007). “Automated reverse engineering of nonlinear dynamical systems”. In: *Proceedings of the National Academy of Sciences* 104.24, pp. 9943–9948.
- Brunton, Steven L, Joshua L Proctor, and J Nathan Kutz (2016). “Discovering governing equations from data by sparse identification of nonlinear dynamical systems”. In: *Proceedings of the National Academy of Sciences* 113.15, pp. 3932–3937.
- Carleo, Giuseppe et al. (2019). “Machine learning and the physical sciences”. In: *Reviews of Modern Physics* 91.4, p. 045002.
- Chen, Yifan et al. (2021). “Solving and learning nonlinear PDEs with Gaussian processes”. In: *Journal of Computational Physics* 447, p. 110668.
- Edelstein-Keshet, Leah (2005). *Mathematical models in biology*. SIAM.
- Genton, Marc G (2001). “Classes of kernels for machine learning: a statistics perspective”. In: *Journal of Machine Learning Research* 2.Dec, pp. 299–312.
- He, Yuchen, Hongkai Zhao, and Yimin Zhong (2022). “How much can one learn a partial differential equation from its solution?” In: *arXiv preprint arXiv:2204.04602*.
- He, Yuchen et al. (2022). “Asymptotic Theory of Regularized PDE Identification from a Single Noisy Trajectory”. In: *SIAM/ASA Journal on Uncertainty Quantification* 10.3, pp. 1012–1036.
- Kaipio, Jari and Erkki Somersalo (2006). *Statistical and computational inverse problems*. Vol. 160. Springer Science & Business Media.
- Kang, Sung Ha, Wenjing Liao, and Yingjie Liu (2021). “IDENT: Identifying differential equations with numerical time evolution”. In: *Journal of Scientific Computing* 87.1, pp. 1–27.
- Karniadakis, George Em et al. (2021). “Physics-informed machine learning”. In: *Nature Reviews Physics* 3.6, pp. 422–440.
- Li, Zongyi et al. (2020). “Fourier Neural Operator for Parametric Partial Differential Equations”. In: *International Conference on Learning Representations*.
- Lu, Lu et al. (2021). “Learning nonlinear operators via DeepONet based on the universal approximation theorem of operators”. In: *Nature Machine Intelligence* 3.3, pp. 218–229.
- Marsden, Jerrold E and Thomas JR Hughes (1994). *Mathematical foundations of elasticity*. Dover Books.
- Muandet, Krikamol et al. (2017). “Kernel mean embedding of distributions: A review and beyond”. In: *Foundations and Trends® in Machine Learning* 10.1-2, pp. 1–141.
- Owhadi, Houman, Clint Scovel, and Gene Ryan Yoo (2021). *Kernel Mode Decomposition and the programming of kernels*. Springer.
- Raissi, Maziar, Paris Perdikaris, and George Em Karniadakis (2019). “Physics-informed neural networks: A deep learning framework for solving forward and inverse problems involving nonlinear partial differential equations”. In: *Journal of Computational Physics* 378, pp. 686–707.
- Riley, Kenneth Franklin, Michael Paul Hobson, and Stephen John Bence (1999). *Mathematical methods for physics and engineering*. Cambridge University Press.
- Rudy, Samuel H et al. (2017). “Data-driven discovery of partial differential equations”. In: *Science Advances* 3.4, e1602614.
- Schaeffer, Hayden (2017). “Learning partial differential equations via data discovery and sparse optimization”. In: *Proceedings of the Royal Society A: Mathematical, Physical and Engineering Sciences* 473.2197, p. 20160446.
- Schmidt, Michael and Hod Lipson (2009). “Distilling free-form natural laws from experimental data”. In: *Science* 324.5923, pp. 81–85.
- Silva, Brian M de et al. (2020). “Pysindy: a python package for the sparse identification of nonlinear dynamics from data”. In: *arXiv preprint arXiv:2004.08424*.
- Stuart, Andrew (2010). “Inverse problems: a Bayesian perspective”. In: *Acta numerica* 19, pp. 451–559.
- Temam, Roger (2001). *Navier-Stokes equations: theory and numerical analysis*. Vol. 343. American Mathematical Society.

- Tröltzsch, Fredi (2010). *Optimal control of partial differential equations: theory, methods, and applications*. Vol. 112. AMS.
- Willard, Jared et al. (2020). “Integrating physics-based modeling with machine learning: A survey”. In: *arXiv preprint arXiv:2003.04919*.